A New Insight into Interface Widths in Binary Polymer Blends Based on Ortho-Positronium Lifetime Studies

P. Ramya, C. Ranganathaiah

Department of Studies in Physics, University of Mysore, Manasagangotri, Mysore 570 006, India

Correspondence to: C. Ranganathaiah (E-mail: cr@physics.uni-mysore.ac.in)

ABSTRACT: The interface widths in two immiscible polymer blend (Poly vinyl chloride (PVC)/Polystyrene (PS)) and PVC/Ethylene Vinyl Acetate (EVA) are determined experimentally using hydrodynamic interaction approach through free volume measurement by positron annihilation lifetime spectroscopy. For comparison, the same study is performed in a miscible blend (Styrene Acrylonitrile (SAN)/Poly Methyl Methacrylate (PMMA)). The interfacial width (Δl) is evaluated from the hydrodynamic interaction (α) based on Kirkwood–Risemann theory and friction coefficient from Stokes equation. Friction at the interface of a binary blend evidences how close the surfaces of the polymer chains come or stay apart which in turn depends on the type of force/interaction at the interface. In this work, we define interface width from a different perspective of Flory–Huggins interaction approach. Measured composition dependent interface widths in the three blends studied clearly demonstrate the sensitivity of the present method. In miscible blend, high friction at the interface results in stronger hydrodynamic interaction and hence smaller interface widths (0.36–1.97 Å), whereas weak or no interaction in immiscible blends produce wider widths (2.81–25.0 Å). © 2012 Wiley Periodicals, Inc. J. Appl. Polym. Sci. 127: 190–199, 2013

INTRODUCTION

Interfaces in polymeric systems exist everywhere in the system. Similar to metallic alloys, we often blend different types of polymers to combine the characteristics of both polymers.[1] The minuscule repulsion between different monomeric units outweighs the entropy gain on mixing of polymers. Thus, the blend phase separates into domains, in which one of the components is enriched relative to the other. Those regions are spatially segregated and are separated by interfaces. On a larger length scale, one can conceive the material as an ensemble of interfaces. Thus, the structure and thermodynamics of internal interfaces between different polymers determine many practically important properties of blends.[2] When a blend just begins to separate into one rich and the other poor domains, the width of the interface is much broader than the molecular size of the polymer;[3] in other words, smaller the width of the interface, more entanglements are formed across these interfaces which improves the mechanical properties of the blend system.[4,5]

Theoretical descriptions, conversely, are quite different to describe interfaces between two unmixed domains.[6–19] The main difference can be traced back to the strength of the interactions on the scale of the monomeric units. In a binary immiscible polymer blend, unfavorable interactions between the component polymers result in large Flory–Huggins parameter. Accordingly, the interface width becomes smaller. In this prescription, however, complex phenomena like roughness of the surfaces, chain end effects at the interface are not included, so the width will be much larger than the size of monomeric unit. In this context, the detailed packing of the monomeric units and the local molecular architecture are important to understand properties of the polymer blends in terms of the interfaces. Generally, interphase or interface width is defined as the third phase in a binary polymer blend enhanced by interdiffusion or compatibilization.[20] However, so far no analytical tool is found suitable for probing these regions so that the actual width can be measured. It is also defined as the region between the adjacent microphases or monomers.[21] In the bilayer polymer thin films, despite the fact that the two layers are immiscible, a narrow region of overlap between two polymers will form. An infinitely sharp interface cannot be formed in any blend system, rather one can say a transition region called the interphase or interface width will be created wherein polymer chain density of one type gradually decreases as the chain density of second type

increases. Therefore, the interface width in a bilayer polymer thin film blend in its defined form cannot be compared to the real blend system with a dispersed phase as it possesses a completely different morphology. The equilibrium interface one finds in real immiscible and partially miscible polymer blends exhibit a profile which varies as a function of volume fraction or segments density of one of the polymer components.

We find several studies reported on the interfacial properties in terms of interdiffusion at the interface,[22–26] interfacial tension,[27–30] and interface width,[21,31–34] and so forth in polymer blends. The magnitude and behavior of interface width with varying molecular weight, temperature, and film thickness have also been studied using the small angle neutron scattering, neutron reflectometry,[27,28,33–35] small angle X-ray scattering, differential scanning calorimetry (DSC),[26] transmission electron microscopy,[30] and so forth with varying success. Schnell et al.[5] had studied interfaces in blends of polystyrene with either poly (p-methylstyrene) or a statistical copolymer poly(styrene-co-p-bromostyrene) using neutron reflection method. Use of two different systems permitted them to study a broad range of interface widths. Blend systems produced from chemical and physical blending process result in three-dimensional morphology and interface characteristics are different from the bilayer interfaces.

The above facts made us interesting to explore the possibility of the method developed recently based on positron lifetime spectroscopy,[36,37] its ability to provide information on the interface widths in dispersed binary polymer blends. As such, in this article, we describe procedure to obtain interface width or its dependence on composition in three dispersed polymer blends; one miscible namely SAN/PMMA and the immiscible blends namely PVC/PS and PVC/EVA with 3D morphology. Further, we have made the analysis of the positron lifetime spectra using two computer routines PATFIT[38] and CONTIN[39] to get discrete components and continuous distribution of lifetimes. This data is used to derive hydrodynamic interaction parameter (α), a concept used for the first time by our group.[36,37] In brief, the concept of hydrodynamic interaction is as follows: the monomer units of dissimilar type in a binary blend produce friction at the interface which stems from the theory of hydrodynamic interaction. This is quantified to understand the behavior of interface regions due to factors like composition. Unlike in the Flory–Huggins interaction, where specific interactions between component polymers are considered responsible for the description of interface, hydrodynamic interaction describes the interface in terms of the friction generated at the interface which certainly owes its compliance to the same interactions. Wolf and coworkers[40,41] reported the effect of hydrodynamic interaction in various polymer/solvent systems based on the KSR[42] and KRZ[43] models. Wolf and coworkers[40,41] theory introduces two parameters namely hydrodynamic interaction parameter (α) and geometric factor (γ) both being evaluated using viscometric data in their work. The γ parameter is expected to depend on the molecular surfaces and volumes in the system, that is, molecular architecture, whereas α is a measure of friction at the interface between the constituents of the blend. This concept was extended to polymer/polymer mixtures in solid phase.[36,37] In this work, the friction at the interface is quantified in terms

of hydrodynamic interaction parameter (α)[36,37,40,41] derived from free volume data obtained from ortho-positronium lifetime measurement. DSC technique is used to supplement positron annihilation lifetime spectroscopy (PALS) results. Scanning electron microscopy (SEM) pictures are just used to show the surface morphology of the samples only. The authors have no intension of making a connection between this morphology and bulk characteristics.

EXPERIMENTAL

Blend Preparation
Samples of SAN (with 25% acrylonitrile), PMMA, PS, PVC, and EVA with densities 1.08, 1.20, 1.04, 1.34, and 0.94 g/cc and weight-average molecular weights 165,000, 15,000, 190,000, 43,000, and 150,000 g/mol, respectively, were procured from M/s Sigma-Aldrich Chemicals. Blends of these samples were prepared by the conventional solvent-casting method. The weighed fractions of SAN and PMMA were dissolved in the common solvent tetrahydrofuran at 60°C in different proportions, (80/20, 50/50, 20/80) in a beaker and kept on a magnetic stirrer, at a temperature of 60°C and continuously stirred with the help of a magnetic bead in the beaker. The stirring was continued till the polymers completely dissolved and a homogenous solution was obtained. The stirring was continued at room temperature until solution reaches room temperature and the solution was cast onto the clean and flat glass plate. The glass plate was kept at room temperature to allow solvent evaporation at room for 24 h. PS and PVC were dissolved in methyl ethyl ketone with wt % 80/20, 50/50, and 20/80 and the solution was cast onto a clean and flat glass plate as described above. Similarly, different proportions (80/20, 50/50, 20/80) of PVC and EVA were dissolved in methyl ethyl ketone and blends were prepared as mentioned above. The neat films were lifted-off from the glass plate. These films were of thickness ≈1 mm for each composition of the blends. Then, the blend samples were vacuum-dried at 70°C for about 10 h to remove the residual solvent. Complete solvent removal was confirmed by measuring constancy in the weight of the samples. All the samples were stored in a desiccator before the experimental usage.

Differential Scanning Calorimetric Measurements
The glass-transition temperatures (T_g) of the homopolymers and their blends were measured with Mettler FP90 DSC instrument connected to liquid nitrogen accessory. Samples of 10 mg were used in the DSC scan with a heating rate of 10°C/min covering the temperature range 40–200°C. The glass transition temperature of the homopolymers and 20/80, 50/50 and 80/20 wt % blends of SAN/PMMA and PVC/PS were determined from DSC scans.

Scanning Electron Microscopy
The surface morphology of the blend samples of SAN/PMMA and PVC/PS (80/20 and 20/80 compositions), with gold coating, were examined using Reith make e-line scanning electron microscope (serial number SUPRA 35-29-77) with 10k resolution.

Positron Annihilation Lifetime Measurements
In brief, the mechanism of positron annihilation is given below: positrons from ^{22}Na radioactive source when injected into a

polymer loses its kinetic energy and reaches thermal energy in a time of the order of pico second. The thermalized positrons annihilate with electrons of the medium through different channels like free annihilation with a lifetime around 0.2 ns or trapped at a defect in the medium and then annihilate with a lifetime of the order of 0.4–0.5 ns. The thermalized positron can also form a bound state called positronium in molecular materials and exists in two allowed spin states: Para-positronium (p-Ps) with spins of e^- and e^+ antiparallel to each other, it annihilates with a mean lifetime of 0.125 ns; The ortho-positronium (o-Ps) (spins of the two particles parallel) has a mean lifetime of 142 ns in vacuum. However, in polymers, the lifetime of o-Ps is shortened to few ns owing to the competing process called pick-off annihilation, in which the positron of o-Ps annihilates by picking an electron of opposite spin from the surrounding medium. As the thermalized o-Ps atoms are localized in cavities or regions of low electron density such as free volume holes of the polymer,[44] the probability of pick-off process is directly related to the electron density of the cavity. Longer o-Ps lifetimes correspond to larger free volume holes, whereas shorter lifetimes correspond to smaller holes.

In this work, the PAL measurements were performed at room temperature using a fast–fast coincidence spectrometer having a time resolution of 0.220 ns. The spectrometer consists of two BaF_2 scintillators and associated electronics.[44,45] A 17μCi ^{22}Na positron source deposited on pure kapton foil of thickness 12.5 μm and source-sample sandwich geometry was used to acquire lifetime spectrum with more than a million counts under each spectrum.

All the PAL spectra obtained were analyzed by two computer routines: (1) finite-term lifetime analysis by PATFIT[38] and (2) continuous-lifetime analysis by CONTIN-PALS2.[39] The finite term lifetime decomposes the PAL spectrum into three discrete lifetime components τ_1, τ_2, and τ_3 with respective intensities I_1, I_2 and I_3, respectively. We attribute these lifetime components as follows: the shortest lifetime τ_1 with intensity I_1 corresponds to p-Ps and free positron annihilations. The lifetime component τ_2 with intensities I_2 is due to trapping of positrons at the defects. The longest lived components τ_3 with intensity I_3 is due to pick-off annihilation of the o-Ps from the free volume sites present mainly in the amorphous regions of the polymer matrix. Nakanishi et al.,[46] relation based on Tao[47] and Eldrup et al.[48] work is used to calculate the free volume cell radius (R) from the measured τ_3 (o-Ps lifetime).

$$\frac{1}{\lambda_3} = \tau_3 = 0.5 \left[1 - \frac{R}{R + \Delta R} + \frac{1}{2\pi} \sin\left(\frac{2\pi R}{R + \Delta R}\right) \right]^{-1} \quad (1)$$

The fitting parameter ΔR is taken as 1.656 Å.[36,37,44,46] The free volume size is evaluated as $V_f = (4/3)\pi R^3$. The fractional free volume or the free volume content (F_v) is calculated as $F_v = CV_f I_3$, where $C = 0.0018$ Å^{-3}.[36,37,44]

The evolution of free volume holes in a polymer results from chain folding and molecular architecture, it is expected that they exhibit a distribution. Therefore, the measured o-Ps lifetime also exhibits a distribution rather than a discrete value.

The CONTIN program provides annihilation rate distributions corresponding to the average discrete values obtained by PATFIT analysis. For CONTIN analysis, well-annealed aluminum spectrum was used as the reference spectrum. We found a good agreement between the mean o-Ps lifetime and intensity obtained by PATFIT and those deduced from CONTIN. More information on data analysis may be obtained from CONTIN program user's manual.[39]

Transformation from annihilation rate probability density function (PDF) into the corresponding free volume radius PDF and free volume size PDF were accomplished by the method of Gregory.[49,50] The expressions used to obtain free volume radius PDF and free volume size PDF are

$$f(R) = 2\Delta R\{\cos[2\pi R/(R + \Delta R)] - 1\}\alpha(\lambda)/(R + \Delta R)^2 \quad (2)$$

$$g(V) = f(R)/4\pi R^2 \quad (3)$$

where ΔR has the same meaning as defined earlier.

RESULTS AND DISCUSSION

DSC Results: Glass Transition Temperature

The glass transition temperature of pure polymers and their blends were determined from DSC scans. A miscible blend results in a single T_g, wherein two T_gs are characteristic of an immiscible binary blend. Figure 1(a) shows the DSC scans for SAN, PMMA, and the SAN/PMMA blends of 80/20, 50/50 and 20/80 composition. In Figure 1(b) shows DSC scans of PVC, PS, and PVC/PS blends of composition 80/20, 50/50, and 20/80. For pure SAN and PMMA polymers, T_g of 100 and 84°C were, respectively, measured. Due to want of space, PVC/EVA blend DSC scans are not shown. The blends SAN/PMMA with composition 80/20, 50/50, and 20/80 exhibit single broad transitions at around 90°C, 87°C, and 85°C, respectively, suggesting miscible nature of the blends. From Figure 1(b), we observe Pure PVC and PS polymers exhibit T_gs around 80 and 103°C, respectively, whereas their blends of composition 80/20, 50/50, and 20/80 show two glass transitions suggesting the immiscible nature of the blends. Although DSC technique is widely used in the miscibility study of polymer blends, it has limitations like when the difference between the T_gs of the constituent polymers is small (<20°C), it is not adequate to resolve them. In such situations, there could be overlap of the T_gs and hence misinterpretation of the data results. Second, DSC is not sensitive to heterogeneities with domain sizes larger than 15 nm. More importantly, DSC results will not provide composition dependent level of miscibility in blends.[20,51]

Surface Morphology

Figure 2(a, b) displays the SEM graphs on the phase morphology of the SAN/PMMA blends of composition 80/20 and 20/80, respectively. The micrographs show almost complete homogeneity and lack discernible domains in the blends. This can be inferred as due to good interaction between the component polymers.

Figure 2(c, d) are the SEM graphs showing the phase morphology of the PVC/PS blends of composition 80/20 and 20/80, respectively. From these scans, it is clear that phase separated
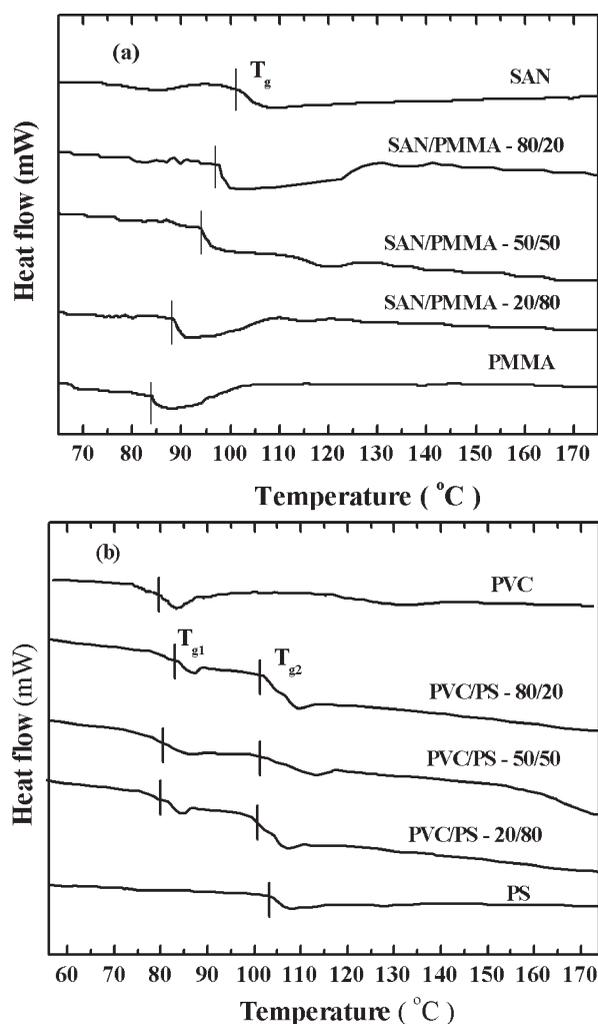
Figure 1. DSC scans of (a) SAN/PMMA blends at different compositions and (b) PVC/PS blends at different compositions.

domains can be seen suggesting incompatibility of the constituent polymers.

Free Volume Results

Miscible blend is a single-phase system representing compact packing of the polymeric segments due to several mechanisms like specific interactions between the functional groups and attractive and repulsive forces among the chains. In terms of free volume, this results in reduced free volume of the blend. Few earlier works used a parameter called interchain interaction parameter to describe the miscibility of polymer blends,[44,45] but it was not adequate to provide any information on the composition dependent miscibility level of the blend. Owing to the limitations of both DSC and inadequacy of the interchain interaction parameter, our group at this laboratory has developed a new method to determine the composition dependent miscibility level in binary polymer blends through hydrodynamic interaction approach making use of the same free volume data.[36,37]

For polymers, viscosity is considered as an important property in understanding the viscoelastic behavior of polymers under stress and strain.[52] Two theories dealing with the flow behavior

of polymer mixtures are one proposed by Rouse[42] based on the works of Kargin and Slonimsky called KSR model and the other by Zimm[43] based on the works of Kirkwood and Risemann called KRZ model. The KSR model assumes polymer molecules as a set of identical elements (segments) or beads connected in series. Further, the linearly connected beads do not disturb the flow rate and hence no perturbation imparted to the motion of the chains. Conversely, the KRZ model is similar in theoretical conceptions of KSR model but brings in the concept of hydrodynamic interaction between the segments of the polymeric chains. This way it accounts for the perturbation of the flow field rates caused by the presence of foreign bodies like the solvent. In principle, two extreme cases are possible; first is polymeric chains do not give rise to perturbations to the flow rate, means no hydrodynamic interaction is present; this limiting case is the KSR model itself, and second, the space occupied by macromolecules is found to be impermeable to the solvent and this corresponds to the maximum possible hydrodynamic interaction.

In case of favorable interactions, the monomers considered as beads in the above theories get closer to each other, therefore, the friction between the chains increases which results to energy dissipation at the interfaces. This excess energy dissipation is revealed by the changes in hydrodynamic interaction parameter (α) of Wolf's theory.[40] In miscible blends, due to attractive interactions between the constituent polymer chains good mixing results and hence friction at the interface is high. Therefore, for miscible blends, α attain large negative values.[36,37,40] For immiscible blends, absence of interactions, α may become zero or positive. Therefore, according to the above prescription, α is a measure of the friction between the surfaces of the beads or monomer units.

From the considerations of the Wolf's theory,[40] the energy dissipation occurs at the molecular interfaces which vary with composition, and hence friction, as flow behavior changes. In this, the energy dissipation is quantified by η the viscosity and shall be governed by the surface fractions of the molecules rather than by their volume or weight fractions. The interrelation between the surface fraction (Ω) and volume fraction (ϕ) of the monomer units is accordingly given by eq. (4), recalled from our earlier work[36,37]

$$\Omega = \frac{(1+\gamma)\phi}{(1+\gamma\phi)} \qquad (4)$$

where γ is a measure of the differences in the ratio of surfaces F and volume V of the monomers of component 1 and 2 and is defined as,

$$\gamma = \frac{F_2/V_2}{F_1/V_1} - 1 \qquad (5)$$

The excess viscosity of the mixture of polymers is defined as

$$\Delta \ln \eta = \ln \eta - (1-\phi)\ln \eta_1 - \phi \ln \eta_2 \qquad (6)$$

Assuming that dissipation of energy takes place at the interfaces between molecular surfaces involving the chains and excluding
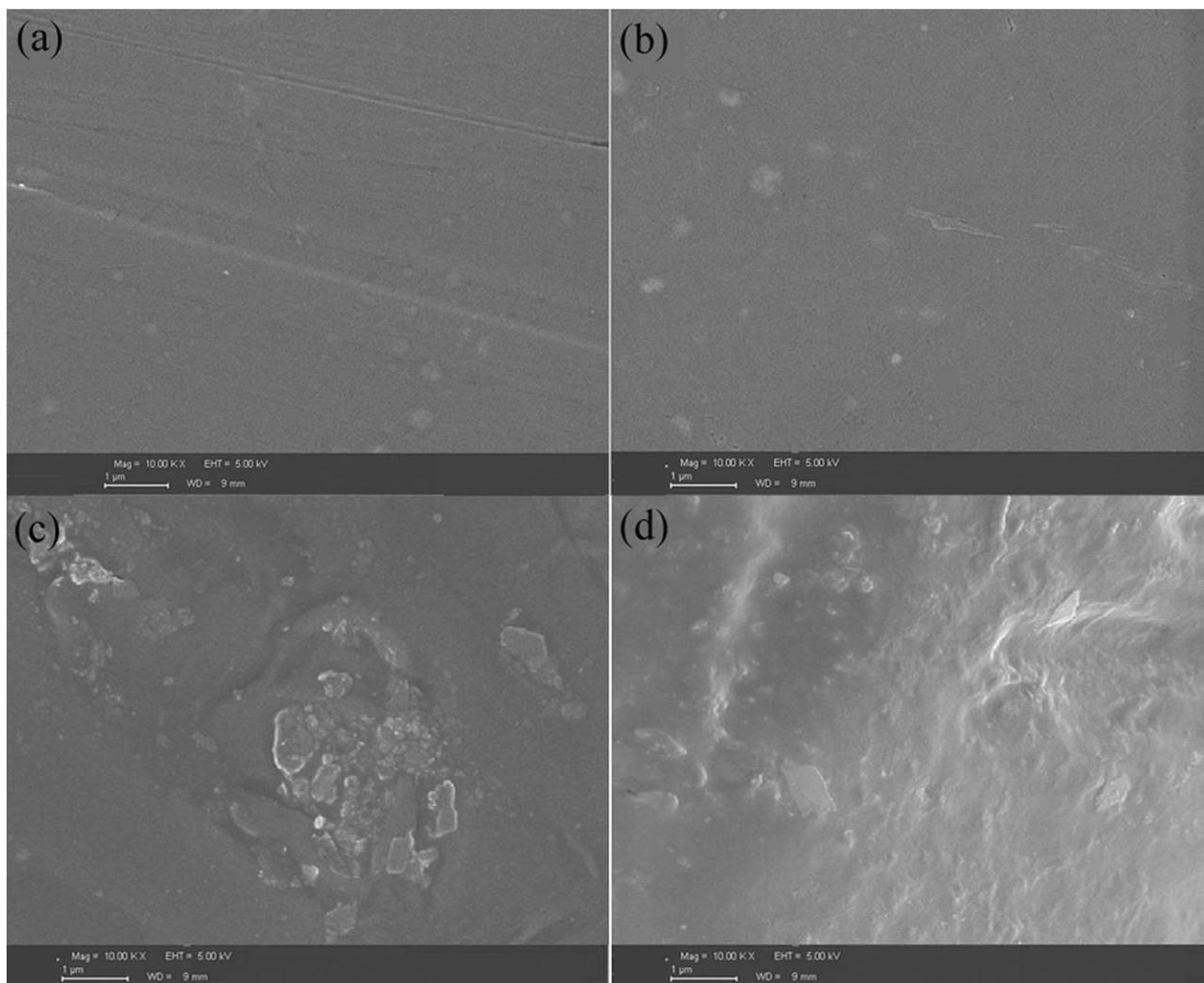
Figure 2. The SEM images of (a) SAN/PMMA(80/20), (b) SAN/PMMA(20/80), (c) PVC/PS(80/20), and (d) PVC/PS (20/80) blend.

specific interactions, one can formulate an ideal mixing law for the viscosity η of the mixture in terms of surface fractions Ω of its components as

$$\ln \eta = \Omega_1^2 \ln \eta_{11} + 2\Omega_1\Omega_2 \ln \eta_{12} + \Omega_2^2 \ln \eta_{22} \quad (7)$$

$\eta_{11} = \eta_1$ and $\eta_{22} = \eta_2$ represent the friction between like molecules and η_{12} measures the mutual friction between unlike components.

The expressions for η_{12} is given by

$$\eta_{12} = \exp[\alpha + m(1 - \Omega)] (\eta_{11}\eta_{22})^{0.5} \quad (8)$$

Here, α is the hydrodynamic interaction. The parameter m accounts for the effects of collective motion; it increases the term in the square bracket of the relation to $(\alpha + m)$ (the correction for nonideal intermolecular friction) in the limit of infinitely dilute solution ($\Omega \to 0$; nondraining coils). Substituting eqs. (7) and (8) in eq. (6) and simplification leads to

$$\Delta \ln \eta = \left\{ \delta[\gamma(1 + \gamma\phi)^2 - (1 - \phi)(1 + \gamma)] \right.$$
$$\left. + 2\alpha(1 + \gamma)^2 \phi + [\eta]\rho (1 - \phi) \right\} \frac{\phi(1 - \phi)}{(1 + \gamma\phi)^3} \quad (9)$$

where δ is determined by the viscosities of the pure components according to the relation

$$\delta = \ln \eta_2 - \ln \eta_1 \quad (10)$$

Wolf et al. argue that thermodynamic preference of contacts between molecules of component 1 (solvent) and component 2 (polymer) leads to reduction of intermolecular friction due to increased tendency of the unlike molecules to move conjointly. This theory has been modified to polymer/polymer system in solid phase[36,37] to evaluate the parameters γ and α using free volume parameters from the measured o-Ps lifetime and intensities; This is done based on the concept that viscosity and free volume are inversely related[53] and polymers in solid phase do exhibit viscoelastic behavior. After simplification of eq. (9) in
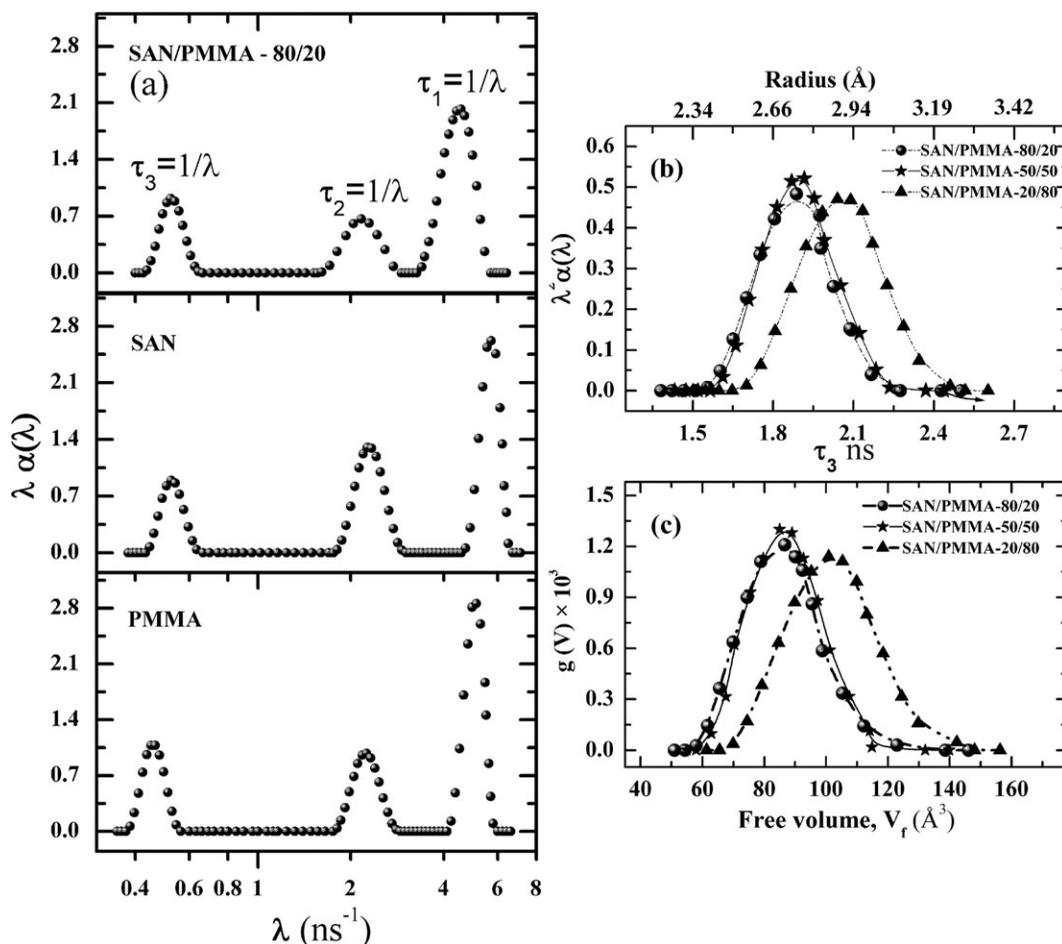
Figure 3. (a) Positron annihilation rate PDF for pure SAN, PMMA, and SAN/PMMA (80/20) blend, (b) plot of (a) *o*-Ps lifetime (τ_3) v/s *o*-Ps probability density function resolved from the lifetime spectra and cavity radius showed in the upper axis, (c) free-volume size (V_f) probability density function for SAN/PMMA blends of 80/20, 50/50, 20/80 compositions.

terms of fractional free volume, we obtain similar expression to that of Wolf et al.

$$\Delta F_V = \left\{ \delta[\gamma(1 + \gamma\,\phi_2)^2 - \phi_1(1 + \gamma)] \right.$$
$$\left. + 2\alpha(1 + \gamma)^2\phi_2 + e^{(1/F_V)}\rho\phi_1 \right\}^{-1} \frac{(1 + \gamma\,\phi_2)^3}{\phi_1\phi_2} \quad (11)$$

where ΔF_v, defined as

$$\Delta F_V = \left[\frac{1}{F_V} - \frac{\phi_1}{F_{V1}} - \frac{\phi_2}{F_{V2}} \right] \quad (12)$$

where F_V is the fractional free volume of the blend, F_{V1} and F_{V2} are the fractional free volumes of the pure polymers, ρ is the density of the blend, ϕ_1 and ϕ_2 are volume fractions of the blend constituents. The γ is expressed as[36,37]

$$F_V = \left[\frac{\phi_1}{F_{V1}} + \frac{\phi_2}{F_{V2}} + \delta\left(\frac{\gamma\phi_1\phi_2}{1 + \gamma\phi_2} \right) \right]^{-1} \quad (13)$$

To evaluate hydrodynamic interaction parameter α, the parameter γ evaluated from eq. (13) are used and eq. (11) is fitted with

the experimental parameters of free volume, volume fractions, and densities. The error estimation on α parameter was also done and found to be around 6%. As described earlier, by monitoring the changes in this parameter, the changes at the interface of the blend can be understood.

Now, we present the free volume results of the bends. In Figure 3(a), we show the positron annihilation rate distribution in SAN, PMMA, and SAN/PMMA (80/20) composition blend obtained from CONTIN analysis of the PAL spectra. Similarly, Figure 4(a) displays positron annihilation rate distribution of PVC, PS, and their 80/20 composition blend sample. In Figure 3(b), the distribution of lifetime and free volume radius, and in Figure 3(c), the free volume size (V_f) distribution are shown for SAN/PMMA blends of 80/20, 50/50, and 20/80 compositions. As can be seen from these figures [Figure 3(b, c)], the distribution of lifetime (τ_3), free volume radius (R), and free volume size (V_f) in 80/20 and 50/50 compositions are narrower (full width at half maximum (FWHM) = 24 $\mathring{A}^3$ and 25 $\mathring{A}^3$, respectively) compared to 20/80 composition (FWHM = 30 $\mathring{A}^3$) and the distribution has shifted toward the PMMA free volume size. The narrower FWHM suggests close packing of the chains in 80/20 and 50/50 composition blends leading to high level of miscibility than for 20/80 composition.
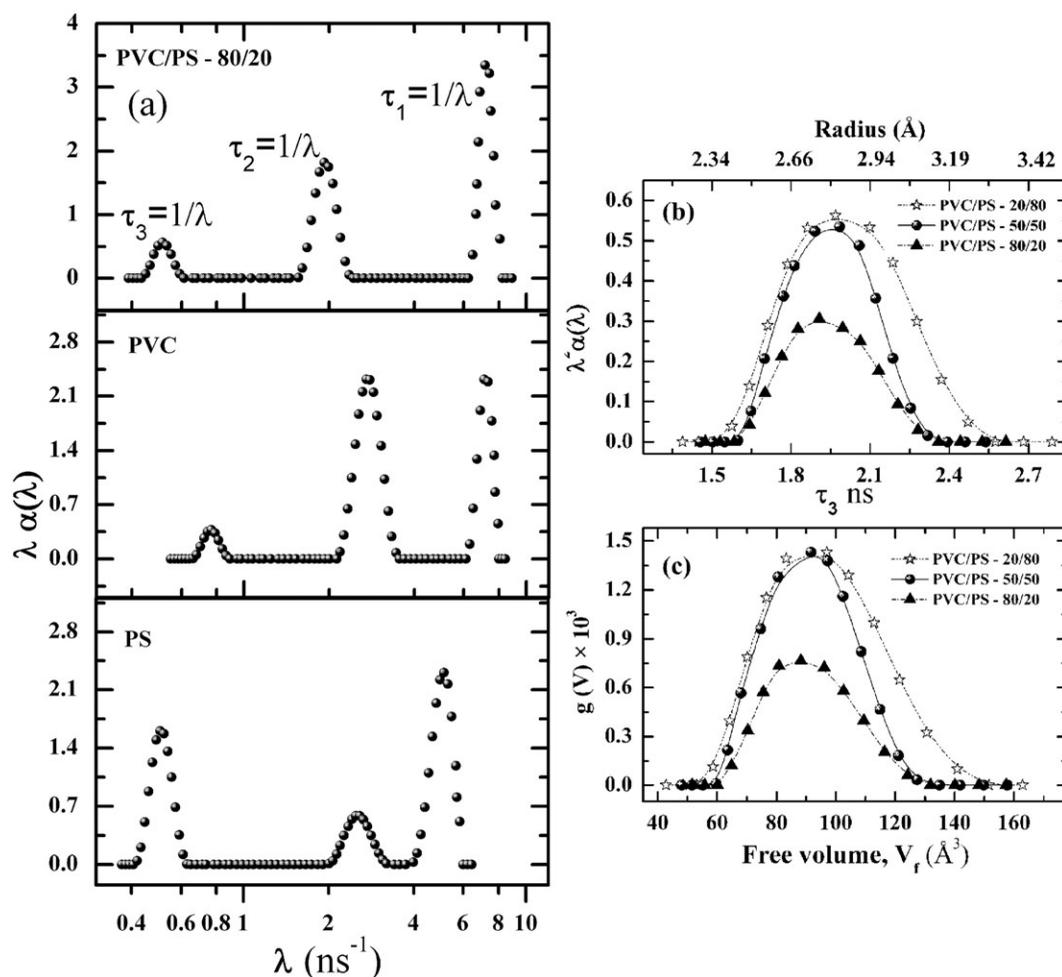
Figure 4. (a) Positron annihilation rate PDF for pure PVC, pure PS, and PVC/PS 80/20 blend, (b) plot of o-Ps lifetime (τ_3) v/s o-Ps probability density function resolved from the lifetime spectra and cavity radius showed in the upper axis, (c) free-volume size (V_f) probability density function for PVC/PS blends of 80/20, 50/50, 20/80 compositions.

For PVC/PS system [Figure 4(b, c)], it can be seen that o-Ps lifetime, free volume radius, and free volume hole size distributions are wider for the 20/80 composition (FWHM = 42 Å^3), whereas 50/50 and 80/20 compositions show narrow (FWHMs 32 and 30 Å^3) distribution. The broad distribution for PVC/PS blends can be inferred as due to additional free volume generated on blending[54] indicating interaction between the component polymers is negligible and hence poor miscibility of the components. However, this will not describe the system fully in the sense what happens at the interface. As such, hydrodynamic interaction concept is brought in and we explore further to get information on the interface width. This is in terms of how close the related surfaces come or how far they are pushed apart due to hydrodynamic interaction and especially in case of immiscible blends. For this, we use α distribution obtained through free volume distribution data to calculate the interface width profile in PVC/PS, PVC/EVA, and SAN/PMMA blends.

For this, the starting point is again Kirkwood and Risemann equations, which connect α parameter to viscosity together with Stokes law for friction.[55] As described earlier, α is a measure of

excess friction generated at the interface in binary polymer blends and is now written as

$$\alpha = \zeta / 8\pi\eta\,\Delta l \tag{14}$$

Here, η is the viscosity of the solvent, Δl is the distance between monomers, and ζ is the friction coefficient. According to Stokes' law, ζ is given by

$$\zeta = 6\pi\eta a \tag{15}$$

where "a" is the monomer radius, and therefore, eq. (14) becomes

Table I. Free Volume Size (V_f), Hydrodynamic Interaction Parameter (α), and Interface Width (Δl) for PVC/PS Blend System

Composition	$V_f \pm 1\%$	$|\alpha| \pm 6\%$	Δl (Å) $\pm 4\%$
80/20	95.2	0.478	3.10
50/50	97.0	0.061	8.10
20/80	96.2	0.006	25.0

Table II. Free Volume Size (V_f), Hydrodynamic Interaction Parameter (α), and Interface Width (Δl) for PVC/EVA Blend System

Composition	$V_f \pm 1\%$	$|\alpha| \pm 6\%$	Δl (Å) $\pm 4\%$
80/20	107.1	0.62	2.81
50/50	119.7	0.41	3.40
20/80	125.7	0.12	6.30

$$\alpha = \frac{3}{4}\left(\frac{a}{\Delta l}\right) \quad (16)$$

This basic equation provides the connection between the dimensions of the monomer unit and how they are moved in or pushed apart depending on the type of interaction or the forces that exist at the interface. For the calculation of the interface width, we further modified the above equation replacing the monomer radius and widths by their respective surface areas and the expression for the interface width Δl now takes the form

$$\Delta l^2 = \frac{3}{4}\left(\frac{a^2}{\alpha}\right); \quad \Delta l = \sqrt{\frac{3a^2}{4\alpha}} \quad (17)$$

Using the $|\alpha|$ values so derived from free volume distributions, the interface widths in PVC/PS, PVC/EVA, and SAN/PMMA blends for different compositions are calculated according to eq. (17) and tabulated in Tables I, II, and III, respectively, along with average V_f values obtained from PATFIT. The following monomer radius (a) values $a_{SAN} = 3.3$ Å, $a_{PMMA} = 2.8$ Å, $a_{PVC} = 2.25$ Å, $a_{EVA} = 2.5$ Å, and $a_{PS} = 2.7$ Å for SAN, PMMA, PVC, EVA, and PS, respectively, were used in the above calculations. It is clear from Table III that for SAN/PMMA blends, as the SAN content decreases the free volume size V_f increases and magnitude of α decreases suggesting that the friction between the polymer chains at the interface decreases. This can be thought as due to the polymer chains pushed apart. This suffice to say that larger the α value, interface width is smaller or narrower and vice versa. This inference holds good to the data in Tables I and II for PVC/PS and PVC/EVA blend systems, which are immiscible at all three compositions.[36,37,56] However, the values of the interface widths reported in Table III are much lower than that reported in the literature (38 nm).[57,58] The reason being that the diffuse interface described in polymer blends in general is based on F–H interaction and this width will be normally wider for miscible blends due to interdiffusion of the component polymer chains at the interface and narrower for immiscible blends. In this prescription, the interface width is defined as the separation between dissimilar chains of the two

Table III. Free Volume Size (V_f), Hydrodynamic Interaction Parameter (α), and Interface Width (Δl) for SAN/PMMA Blend System

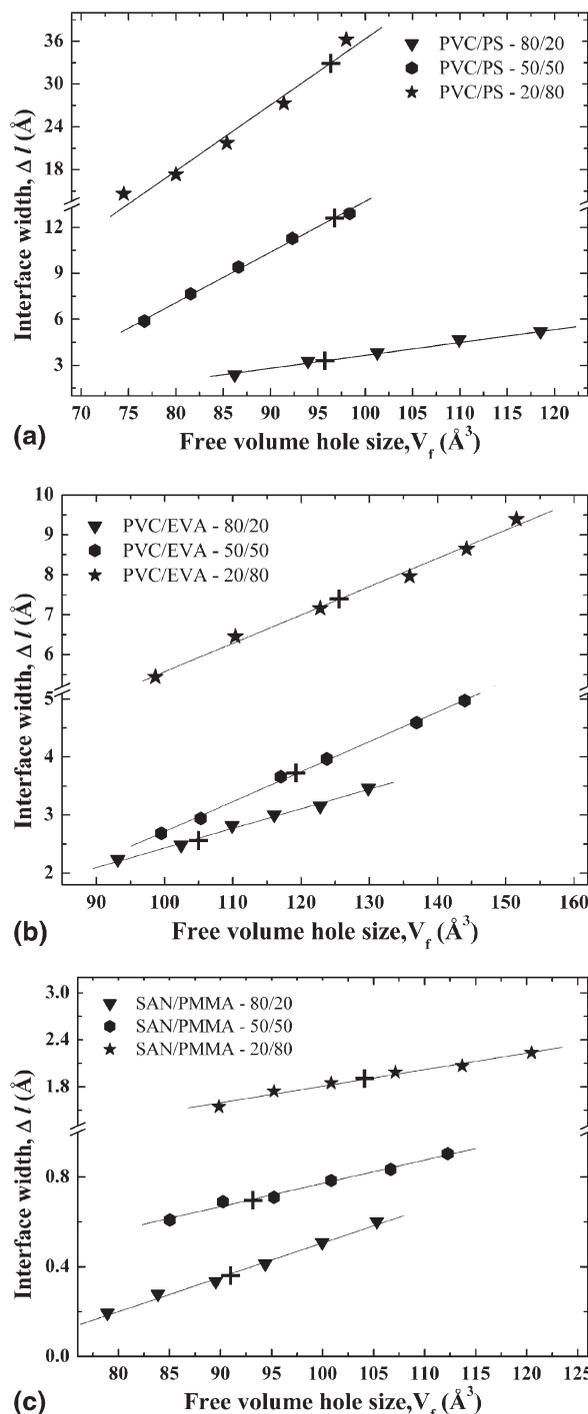| Composition	$V_f \pm 1\%$	$|\alpha| \pm 6\%$	Δl (Å) $\pm 4\%$
80/20	90.0	63.4	0.36
50/50	92.0	12.4	0.82
20/80	103.0	2.15	1.97

Figure 5. (a) Plot of free volume hole size (V_f) of the blend and interface width Δl for PVC/PS blends for different compositions (correlation coefficient $R = 0.999$) + mark on the curves indicate the V_f values of the blend obtained from PATFIT analysis indicating good agreement with CONTIN analysis results. (b) Plot of free volume hole size (V_f) of the blend and interface width Δl for PVC/EVA blends for different compositions, (correlation coefficient $R = 0.99$). + Mark on the curves indicate the V_f values of the blend obtained from PATFIT analysis indicating good agreement with CONTIN analysis results. (c) Plot of free volume hole size (V_f) of the blend and interface width Δl for SAN/PMMA blend for different compositions (correlation coefficient $R = 0.98$) + mark on the curves indicate the V_f values of the blend obtained from PATFIT analysis indicating good agreement with CONTIN analysis results.

component polymers obtained in terms of friction at the interface. We justify this argument because hydrodynamic interaction concept is well accepted like Flory–Huggins interaction.[55,59] No interactions between components of immiscible blends produce large values for F–H interaction parameter (polymer/solvent system) and hence interface width will be small but for similar blends like PVC/PS and PVC/EVA, hydrodynamic interaction gives a larger width. In the F–H prescription, complex processes like surface roughness, chain ends at the interface are not included. Conversely, the hydrodynamic interaction formalism deals with surfaces of monomer units of component polymers and their characteristic behavior at the interface. In fact, this process better describes the evolution of free volume due to chain ends and folding. The interface widths in PVC/PS and PVC/EVA immiscible blends are wider compared to narrow widths in completely miscible SAN/PMMA system. As the formulation of hydrodynamic theory excludes specific interactions between the polymer components, the description here is in terms of the separation of the chains at the interface.

Further, from the CONTIN analysis of o-Ps lifetimes, we have generated the distribution of α at the interface for each composition of the three blend systems. The purpose is to see how the hydrodynamic interaction varies across the interface, as no clear boundary exists in reality between the two polymer chains and segments. We have constructed plots of V_f values against the interface width derived from CONTIN analysis results in exactly the same way that was done with PATFIT data. These are shown in Figure 5(a–c) for PVC/PS, PVC/EVA, and SAN/PMMA blends, respectively. The data fit to a linear relationship (with $R = 0.99$). What is clear from these graphs is that as the free volume cell size increases across the interface, the interface width also increases. It is to be noted that the SAN/PMMA blend is known to be miscible not because of the intermolecular interactions but because of the intramolecular repulsion between the SAN chains and PMMA chains easily slide in between the SAN chains.[60,61]

CONCLUSIONS

On the basis of above discussion, the following conclusions can be arrived at

- The distribution PDFs for the free volume parameters provide better understanding of the interface characteristics in binary blend systems compared with discrete lifetime analysis.
- The concept of hydrodynamic interaction has been shown to be very useful and provides a new insight into interface width in real immiscible polymer blends.
- The interface widths measured are of the order of few angstroms (2.81–25 Å) in immiscible blends larger than in miscible blend. With hydrodynamic interaction concept, the friction at the interface determines the interface width.

ACKNOWLEDGMENTS

REFERENCES

1. Paul, D. R.; Newman, S. Polymer Blends; Academic: New York, **1978.**
2. Stamm, M.; Schubert, D. W. *Ann. Rev. Mater. Sci.* **1995,** *25*, 325.
3. Tucker, C. L.; Moldenaers, P. *Ann. Rev. Fluid Mech.* **2002,** *34*, 177.
4. Brown, H. R.; Char, K.; Deline, V. R.; Green, P. F. *Macromolecules* **1993,** *26*, 4155.
5. Schnell, R.; Stamm, M.; Creton, C. *Macromolecules* **1999,** *32*, 3420.
6. Helfand, E.; Tagami, Y. *J. Chem. Phys.* **1972,** *56*, 3592.
7. Helfand, E. *J. Chem. Phys.* **1975,** *62*, 999.
8. Scheutjens, J. M.; Fleer, G. J. *J. Phys. Chem.* **1979,** *83*, 1619.
9. Noolandi, J.; Hong, K. M. *Macromolecules* **1981,** *14*, 727.
10. Shull, K. R. *Macromolecules* **1993,** *26*, 2346.
11. Szleifer, I.; Carignano, M. A. Tethered Polymer Layers: Adv. Chem. Phys., 94, Wiley: New York, **1996.**
12. Matsen, M. W.; Schick, M. *Phys. Rev. Lett.* **1995,** *74*, 4225.
13. Woodward, C. E. *J. Chem. Phys.* **1991,** *94*, 3183.
14. Woodward, C. E.; Yethiraj, A. *J. Chem. Phys.* **1995,** *102*, 5499.
15. Yethiraj, A. *J. Chem. Phys.* **1998,** *109*, 3269.
16. Müller, M.; MacDowell, L. G. *Macromolecules* **2000,** *33*, 3902.
17. Müller, M.; MacDowell, L. G.; Yethiraj, A. *J. Chem. Phys.* **2003,** *118*, 2929.
18. Müller, M.; Schmid, F. *Adv. Polym. Sci.* **2005,** *185*, 1.
19. Patra, C. N.; Yethiraj, A. *J. Chem. Phys.* **2003,** *118*, 4702.
20. Utracki, L. A. Polymer Alloys and Blends—Thermodynamics and Rheology; Hanser: New York, **1990.**
21. Anastasiadis, S. H.; Russell, T. P.; Satija, S. K.; Majkrzak, C. F. *J. Chem. Phys.* **1990,** *92*, 5677.
22. Kim, W. C.; Pak, H. *Bull. Korean Chem. Soc.* **1999,** *20*, 1323.
23. Sung, Y. T.; Seo, W. J.; Kim, Y. H.; Lee, H. S.; Kim, W. N. *Korea-Australia Rheol. J.* **2004,** *16*, 135.
24. Dlubek, G.; Pionteck, J.; Bondarenko, V.; Pompe, G.; Taesler, C.; Petters, K.; Krause- Rehberg, R. *Macromolecules* **2002,** *35*, 6313.
25. Dlubek, G.; Pompe, G.; Pionteck, J.; Janke, A.; Kilburn, D. *Macromol. Chem. Phys.* **2003,** *204*, 1234.
26. Dlubek, G.; Bondarenko, V.; Pionteck, J.; Kilburn, D.; Pompe, G.; Taesler, C.; Redmann, F.; Petters, K.; Rehberg, R. K.; Alam, M. A. *Rad. Phys. Chem.* **2003,** *68*, 369.
27. Anastasiadis, S. H.; Gancarz, I.; Koberstein, J. T. *Macromolecules* **1988,** *21*, 2980.
28. Broseta, D.; Fredrickson, G. H.; Helfand, E.; Leibler, L. *Macromolecules* **1990,** *23*, 132.
29. Jain, T. S.; de Pablo, J. J. *J. Chem. Phys.* **2003,** *118*, 4226.
30. Liao, Y.; Nakagawa, A.; Horiuchi, S.; Ougizawa, T. *Macromolecules* **2007,** *40*, 7966.

31. Schubert, D. W.; Stamm, M. *Europhys. Lett.* **1996,** *35*, 419.

32. Sferrazza, M.; Xiao, C.; Bucknall, D. G.; Jones, R. A. L. *J. Phys. Condens. Matter* **2001,** *13*, 10269.

33. Careli, C.; Young, R. N.; Jones, R. A. L.; Sferrazza, M. *Europhys. Lett.* **2006,** *75*, 274.

34. Carelli, C.; Jones, R. A. L.; Young, R. N.; Cubitt, R.; Krastev, R.; Gutberlet, T.; Dalgliesh, R.; Schmid, F.; Sferrazza, M. *Europhys. Lett.* **2005,** *71*, 763.

35. Beziel, W.; Frgneto, G.; Cousin, F.; Sferrazza, M. *Phys. Rev. E* **2008,** *78*, 022801.

36. Ranganathaiah, C.; Kumaraswamy, G. N. *J. Appl. Polym. Sci.* **2009,** *111*, 577.

37. Raj, J. M.; Ranganathaiah, C. *J. Polym. Sci. Part B: Polym. Phys.* **2009,** *47*, 619.

38. Kirkegaard, P.; Pederson, N. J.; Eldrup, M.; *Riso Nat Lab Reports, Denmark M-2740,* **1989.**

39. Gregory, R. B. CONTIN(PALS-2) CONTIN (PAL-2): a Modification of CONTIN (Version2) for the Determination of Positron Annihilation Lifetime Distributions. Kent State University: USA, **1993.**

40. Schnell, M.; Wolf, B. A. *J. Rheol.* **2000,** *44*, 617.

41. Mertsch, R.; Wolf, B. A. *Ber. Bunsenges Phys. Chem.* **1994,** *98*, 1275.

42. Rouse, P. J. *J. Chem. Phys.* **1953,** *21*, 1272.

43. Zimm, B. *J. Chem. Phys.* **1956,** *24*, 269.

44. Jean, Y. C. *Michrochem. J.* **1990,** *42*, 72.

45. Ravikumar, H. B.; Ranganathaiah, C.; Kumaraswamy, G. N.; Thomas, S. *Polymer* **2005,** *46*, 2372.

46. Nakanishi, H.; Wang, S. J.; Jean, Y. C. In Proceedings of the International Symposium on Positron Annihilation in Fluids, S. C. Sharma Ed. World Scientific: Singapore, 292, **1988.**

47. Tao, S. J. *J. Chem. Phys.* **1972,** *56*, 5499.

48. Eldrup, M.; Lightbody, D.; Sherwood, J. N. *Chem. Phys.* **1981,** *63*, 51.

49. Provencher, S. W. *Comput. Phys. Commun.* **1982,** *27*, 229.

50. Gregory, R. B. *J. Appl. Phys.* **1991,** *70*, 4665.

51. Olabisi, O.; Robeson, L.; Shaw, M. T. Polymer-Polymer Miscibility; Academic: New York, **1970.**

52. Riande, E.; Diaz-Calleja, R.; Prolongo, M. G.; Masegosa, R. M.; Salom, C. Polymer Viscoelasticity: Stress and Strain in Practice; Marcel Dekker: New York, **2000.**

53. Williams, M. L.; Landel, R. F.; Ferry, J. D. *J. Am. Chem. Soc.* **1995,** *77*, 3701.

54. Liu, J.; Jean, Y. C.; Yang, H. *Macromolecules* **1995,** *28*, 5774.

55. Zwanzig, R.; Kiefer, J.; Weiss, G. H. *Proc. Natl. Acad. Sci.* **1968,** *60*, 381.

56. Abd-El-Messieh, S. L. *Polym. Plast. Technol. Eng.* **2003,** *42*, 153.

57. Li, X.; Li, W.; Hoffmann, G. G.; Goossens, G. P. J.; Loos, J.; With, G. *Macromolecules* **2011,** *44*, 2852.

58. Horiuchi, S.; Yin, D.; Liao, Y.; Ougizawa, T. *Macromol. Rapid Commun.* **2007,** *28*, 915.

59. Stamm, M. Polymer Surfaces and Interfaces—Characterization, Modification and Applications; Springer: Verlag Berlin Heidelberg, **2007.**

60. Robertson, C. G.; Wilkes, G. L. *Polymer* **2001,** *42*, 1581.

61. Fowler, M. E.; Barlow, J. W.; Paul, D. R. *Polymer* **1987,** *28*, 1177.